

ANL/ET/CP-98334

## OXIDATION PERFORMANCE OF V-Cr-Ti ALLOYS\*

K. Natesan and M. Uz  
Fusion Power Program  
Argonne National Laboratory  
Argonne, IL 60439 USA

February 2000

The submitted manuscript has been created by the University of Chicago as Operator of Argonne National Laboratory ("Argonne") under Contract No. W-31-109-ENG-38 with the U.S. Department of Energy. The U.S. Government retains for itself, and others acting on its behalf, a paid-up, nonexclusive, irrevocable worldwide license in said article to reproduce, prepare derivative works, distribute copies to the public, and perform publicly and display publicly, by or on behalf of the Government.

RECEIVED  
MAY 03 2000  
OSTI

Presented at the 5th International Symposium on Fusion Nuclear Technology, Sept. 19-24, 1999, Rome.

\*Work supported by Office of Fusion Science, U.S. Department of Energy, under Contract No. W-31-109-Eng-38.

## **DISCLAIMER**

**This report was prepared as an account of work sponsored by an agency of the United States Government. Neither the United States Government nor any agency thereof, nor any of their employees, make any warranty, express or implied, or assumes any legal liability or responsibility for the accuracy, completeness, or usefulness of any information, apparatus, product, or process disclosed, or represents that its use would not infringe privately owned rights. Reference herein to any specific commercial product, process, or service by trade name, trademark, manufacturer, or otherwise does not necessarily constitute or imply its endorsement, recommendation, or favoring by the United States Government or any agency thereof. The views and opinions of authors expressed herein do not necessarily state or reflect those of the United States Government or any agency thereof.**

## DISCLAIMER

Portions of this document may be illegible in electronic Image products. Images are produced from the best available original document

# OXIDATION PERFORMANCE OF V-Cr-Ti ALLOYS

K. Natesan and M. Uz

Fusion Power Program, Argonne National Laboratory, Argonne, IL 60439 USA

## Abstract

Vanadium-base alloys are being considered as candidates for the first wall in advanced V-Li blanket concepts in fusion reactor systems. However, a primary deterrent to the use of these alloys at elevated temperatures is their relatively high affinity for interstitial impurities, i.e., O, N, H, and C. We conducted a systematic study to determine the effects of time, temperature, and oxygen partial pressure ( $pO_2$ ) in the exposure environment on O uptake, scaling kinetics, and scale microstructure in V-(4-5) wt.% Cr-(4-5) wt.% Ti alloys. Oxidation experiments were conducted on the alloys at  $pO_2$  in the range of  $5 \times 10^{-6}$ -760 torr ( $6.6 \times 10^{-4}$ - $1 \times 10^5$  Pa) at several temperatures in the range of 350-700°C.

Models that describe the oxidation kinetics, oxide type and thickness, alloy grain size, and depth of O diffusion in the substrate of the two alloys were determined and compared. Weight change data were correlated with time by a parabolic relationship. The parabolic rate constant was calculated for various exposure conditions and the temperature dependence of the constant was described by an Arrhenius relationship. The results showed that the activation energy for the oxidation process is fairly constant at  $pO_2$  levels in the range of  $5 \times 10^{-6}$ -0.1 torr. The activation energy calculated from data obtained in the air tests was significantly lower, whereas that obtained in pure-O tests (at 760 torr) was substantially higher than the energy obtained under low- $pO_2$  conditions. The oxide  $VO_2$  was the predominant phase that formed in both alloys when exposed to  $pO_2$  levels of  $6.6 \times 10^{-4}$  to 0.1 torr.  $V_2O_5$  was the primary phase in specimens exposed to air and to pure  $O_2$  at 760 torr. The implications of the increased O concentration are increased strength and decreased ductility of the alloy. However, the strength of the alloy was not a strong function of the O concentration of the alloy, but an increase in O concentration did cause a substantial decrease in ductility.

## 1. Introduction

Vanadium-base alloys that nominally contain 4-5 wt.% chromium and 4-5 wt.% titanium have been identified as the most viable materials for fusion reactor applications because their long-term activation, irradiation afterheat, biological hazard potential, and thermal stress factor are lower, and their creep resistance, compatibility with coolants such as liquid alkali metals, and mechanical formability are better than those for other structural materials. A primary deterrent to the use of V-base alloys at elevated temperatures is their relatively high affinity for interstitial impurities, i.e., O, N, H, and C. In particular, O (the subject of this paper) may degrade alloy properties during service through dissolution in the matrix or formation of oxide particles in the matrix, along the grain boundaries, and/or on the surface of the

alloys. Therefore, a good understanding of the oxidation behavior of alloys intended for use at elevated temperatures is of significant importance.

Earlier oxidation studies in our laboratory were conducted on V-5Cr-5Ti (designated as 55) alloy specimens at several temperatures in an air environment [1,2]. The oxidation process followed a parabolic rate law. The oxide scale exhibited a dual layer, with the outer layer predominantly V oxide and the inner layer (V,Ti) oxide. Subsequently, another study was conducted to determine and compare the air-oxidation behavior of V-4Cr-4Ti (designated as 44) and 55 alloys in the temperature range of 300-650°C [3]. Models that describe the oxidation kinetics, oxide type and thickness, alloy grain size, and depth of O diffusion in the substrate of the two alloys were determined and compared. From the results that were obtained, we reached the following conclusions:

- The oxide that formed on either alloy was predominantly  $V_2O_5$ ; also, some  $VO_2$  and/or a complex (V, Cr, Ti) oxide was possibly present.
- Oxide scales on both alloys were continuous and tenacious, and the oxidation kinetics followed a parabolic or nearly parabolic nonlinear growth rate law.
- Alloy 55 was consistently more oxidation-resistant than Alloy 44, and the difference in their oxidation resistance increased with increasing temperature above 500°C.
- Oxygen diffusion was faster in Alloy 44 than in Alloy 55. However, the activation energies of diffusion of oxygen in both alloys were within 5% of one another.
- The microstructures of both alloys were quite stable, because no measurable grain growth was observed in either after 2100 h at 500°C or after  $\approx 200$  h at 650°C.

This paper examines the oxidation performance of Alloys 44 and 55 at temperatures between 350 and 700°C in an air environment and in O environments with pressures in a range of  $5 \times 10^{-6}$ -760 torr. Extensive microstructural analyses of the O-exposed specimens were conducted to evaluate the oxide morphology and oxide scale thicknesses. Models, developed earlier to describe the oxidation kinetics in air, were extended to oxidation in low- $pO_2$  environments. In addition, Vickers hardness profiles of oxygenated alloys were obtained to characterize the influence of O ingress on the hardening of the alloys.

## 2. Experimental Procedure

The compositions of the V-Cr-Ti alloys that we selected for the study are given in Table 1. Both Alloys 44 and 55 were obtained as 1-mm-thick cold-rolled sheets. A sheet material of each alloy was annealed for 1 h at 1050°C at  $\approx 10^{-6}$  torr before it was used in oxidation tests. Initial grain size of the Alloy 44 and 55 specimens was  $\approx 20$  and 32  $\mu\text{m}$ , respectively. Grain size measurements showed virtual absence of grain growth in both alloys at 500, 650, and 800°C after  $\approx 5000$  h. Coupon specimens  $\approx 15 \times 7.5 \times 1$  mm were used for the oxidation studies. Our earlier work on oxidation of these alloys was conducted in air in a thermogravimetric test apparatus (TGA) at 300-650°C [1-3]. Oxidation experiments in 760-torr  $O_2$  environments were conducted in a similar manner (i.e., continuous weight measurements) in a TGA at temperatures between 400 and 700°C. Temperatures were maintained within  $\pm 2^\circ\text{C}$  of the

desired value. The exposures in environments with low oxygen partial pressure ( $pO_2$ ) were conducted in an apparatus in which pure  $O_2$  gas was used in a feed/bleed manner to maintain the desired  $O$  pressure in the range of  $5 \times 10^{-6}$ -0.1 torr. No carrier gas was used in the low-  $pO_2$  experiments. In these experiments, specimens were retrieved periodically and weighed, and dimensions were measured. The oxidation products were examined by X-ray diffraction (XRD) analysis, and the scale microstructures were evaluated by scanning electron microscopy (SEM) and energy-dispersive X-ray analysis. In addition, microhardness was measured on cross sections of exposed specimens to obtain hardness profiles and correlate them with  $O$  concentration in the alloys. Vickers hardness values were obtained by applying a load of 100 gf and by measuring the size of the resulting unrecovered indentation by using a microscope.

Tensile specimens of both alloys were fabricated according to ASTM specifications and had a gauge length of  $\approx 19$  mm and a gauge width of  $\approx 4.5$  mm. Before any further treatment or testing, all tensile samples were annealed for 1 h at  $1050^\circ C$  under a pressure of  $\approx 10^{-6}$  torr. Specimens of both alloys were exposed to several environments with  $pO_2$  in a range of  $1 \times 10^{-6}$ -760 torr for 250-275 h at  $500^\circ C$  and were subsequently tensile-tested at a strain rate of  $1.8 \times 10^{-4} s^{-1}$  in air at room temperature or  $500^\circ C$ . Total elongation was measured with a vernier caliper and by using load/elongation chart records. Fracture surfaces and polished surfaces in longitudinal and axial directions in the vicinity of fracture region of tested specimens were examined by SEM.

### 3. Results and Discussion

Extensive studies were conducted on the oxidation kinetics of Alloys 44 and 55 in air over a temperature range of  $300$ - $650^\circ C$ ; the results were reported earlier [1-3]. The current oxidation study on the two alloys involved exposure of the alloys to low- $pO_2$  and 100 vol.%  $O_2$  environments. Table 2 lists the experimental variables, such as  $pO_2$  in the exposure environment and test temperature, that were used in several of the experiments on the two alloys. Figure 1 shows normalized weight changes (in  $mg/mm^2$ ) for Alloys 44 and 55 after exposure at 500, 600, and  $700^\circ C$  in several low- $pO_2$  environments. The figure also shows data at 450, 525, and  $600^\circ C$  that were obtained for the alloys after exposures in a 760-torr  $O_2$  atmosphere. The exposure temperature in a 100 vol.%  $O_2$  atmosphere was limited to  $600^\circ C$  because the  $V_2O_5$  scale that forms in this environment melts at  $670^\circ C$ .

The weight change data were correlated with time by the parabolic relationship  $w^2 = k_p \cdot t$ , where  $w$  is weight change,  $t$  is exposure time, and  $k_p$  is a parabolic rate constant. The  $k_p$  values calculated for various exposure conditions are also listed in Table 2. Figure 2 shows the temperature dependence of the parabolic rate constant for the two alloys exposed to various  $O$  pressures. The temperature dependence of the parabolic rate constant is described by the relationship  $k_p = k_0 \exp[-Q/(RT)]$ , where  $k_0$  is a preexponential term,  $Q$  is the activation energy for the oxidation process,  $R$  is a gas constant, and  $T$  is absolute temperature. The values for  $k_0$  and  $Q$ , calculated from the best fit of the experimental data at various  $O$  pressures, are also listed in Table 2. The results show that the activation energy for the oxidation process is fairly constant at  $O$  pressures of  $10^{-6}$  to  $10^{-1}$  torr. The activation energy calculated

from data in the air tests was significantly lower, and in pure-O tests (at 760 torr), was substantially higher than the values obtained under low-pO<sub>2</sub> conditions. It is not clear at present whether the type of scale (predominantly V<sub>2</sub>O<sub>5</sub>) that forms in air and in pure O<sub>2</sub> is the cause for this difference.

Table 3 lists the XRD data obtained on the oxidation products from several specimens exposed to various O pressures. The oxide VO<sub>2</sub> was the predominant phase in both alloys when exposed to pO<sub>2</sub> in the range of  $5 \times 10^{-6}$  to  $10^{-1}$  torr; V<sub>2</sub>O<sub>5</sub> was the primary phase in specimens exposed to air and to pure O<sub>2</sub> at 760 torr. The XRD spectra indicated only a weak possibility of Ti- or Cr-containing oxides, even though Ti is a stronger oxide former than V.

Cross sections of several of the exposed specimens were examined by SEM. The results showed that the initial grain size of Alloy 44 is smaller than that for Alloy 55 and furthermore, the grain size of both alloys changes very little, even after exposure for  $\approx 185$  h at 700°C in an O<sub>2</sub> environment at  $5 \times 10^{-6}$  torr. This observation is consistent with data reported earlier on grain growth in Alloy 44 in the temperature range of 500-1000°C [4]. Analysis of the cross section of the scale/alloy interface region for Alloys 44 and 55 after exposure at 700°C to an O<sub>2</sub> environment at  $5 \times 10^{-6}$  torr indicated that the oxide layers in both alloys were continuous and tenacious. The tenacity of the oxide was also evident from the lack of spalling during handling of the oxidized samples of both alloys. The oxide thickness of both alloys was on the order of 1-2  $\mu\text{m}$  and predominantly consisted of VO<sub>2</sub>. The near-surface regions of both alloys exhibited some cracking, indicative of the brittleness of the alloy caused by oxygen enrichment.

Figure 3 shows the Vickers hardness profiles of the Alloy 44 specimen after exposure at 500, 600, and 700°C in several low-pO<sub>2</sub> environments and for Alloys 44 and 55 after exposure to 760-torr O<sub>2</sub> at 600°C. After exposure at 500°C, the profiles showed negligible variation in hardness across the entire cross section of the specimen in all of the low-pO<sub>2</sub> environments, indicating that the scale thickness is extremely thin (1-2  $\mu\text{m}$ ) and the O penetration into the alloy is negligible during the exposure period in the range of 200-400 h (see Fig. 1 for exposure times). At 600°C, the profiles showed an increase in hardness in the surface region of the specimens after exposure in all of the environments that were studied. Irrespective of pO<sub>2</sub> in the range of  $5 \times 10^{-6}$  to 760 torr in the exposure environment, the thickness of the hardened layer was  $\approx 0.2$  mm in all of the specimens that were exposed at 600°C. The hardness profiles indicate a substantial enrichment in O concentration over the entire cross section of the 1-mm-thick specimen after exposure at 700°C, irrespective of pO<sub>2</sub> in the range of  $5 \times 10^{-6}$ -0.1 torr in the exposure environment.

Based on the activation energy of 130 kJ/mole and D<sub>0</sub> value of 0.0145 m<sup>2</sup>/h for diffusion in Alloy 44, derived from oxidation data obtained in an air environment ( Ref. 3), the diffusion coefficient for O in the alloy should be  $2.38 \times 10^{-11}$ ,  $2.41 \times 10^{-10}$ , and  $1.52 \times 10^{-9}$  m<sup>2</sup>/h at 500, 600, and 700°C, respectively. Based on the specimen exposure times of 175 h at 700°C, oxygen penetration is such that the center of the specimen would have attained  $\approx 90\%$  of the surface concentration, which is in fair agreement with the data on earlier hardness profiles. Similar calculations for exposure at 600°C showed that the center

should have attained  $\approx 18\%$  of the surface concentration during the exposure time of  $\approx 195$  h used in the present studies. This discrepancy may arise because a smaller activation energy value is derived from air-exposure data or because the correlation of hardness with O concentration is not sensitive enough at given O levels. Another possible cause for this discrepancy is the trapping of O by Ti or precipitation of Ti-rich oxides in the alloy. Chemical analysis of air-exposed specimens indicated negligible N enrichment of the specimens, implying that N does not contribute to the increased hardness. Furthermore, in a low- $pO_2$  exposure environment, N species were not present during the exposure of the specimens. At  $500^\circ\text{C}$ , the calculations showed that the center would not be affected and the depth of penetration of O into the alloy would be  $\approx 0.15$  mm from either side. Hardness profiles at  $500^\circ\text{C}$  do not confirm such a penetration, probably because of the insensitivity of hardness to O at low levels.

The implications of the increased O concentration are increased strength and decreased ductility of the alloy. However, the strength of the alloy has not been a strong function of its O concentration but an increase in O concentration causes a substantial decrease in alloy ductility. Extensive tensile tests have been conducted with specimens that have been exposed to air and low- $pO_2$  environments and some of the results were reported in earlier papers [1, 2, 4]. Because O uptake by the alloys is predominantly a diffusion process, the O concentration is strongly influenced by exposure temperature and time and the section thickness of the alloy. Table 4 summarizes uniform- and total-elongation data that were obtained from tensile tests on Alloys 44 and 55 that had been exposed at 500 and  $700^\circ\text{C}$  for  $\approx 250$  h to various concentrations of O. The results show that the ductility of the alloys after a 250-h exposure at  $500^\circ\text{C}$  did not decrease the elongation values significantly, primarily because the diffusion coefficient for O in the alloys is low enough at  $500^\circ\text{C}$  that the exposure time of 250 h did not significantly increase the O uptake of the alloys. For the specimens exposed at  $700^\circ\text{C}$ , the penetration of O being substantial during a 250-h exposure, the decrease in elongation values is substantial; and, in most cases, these values are close to zero, even at the elevated test temperatures of 500 and  $700^\circ\text{C}$  and low  $pO_2$  of  $1 \times 10^{-6}$  torr in the exposure environment.

#### **4. Summary**

A systematic study was conducted to evaluate the oxidation kinetics of V-(4-5)Cr-(4-5)Ti alloys at temperatures in the range of  $400\text{-}700^\circ\text{C}$  in an air environment and in O with pressures in a range of  $5 \times 10^{-6}$  to 760 torr. Several conclusions can be drawn from the investigation.

The oxidation process and oxygen uptake of the V-Cr-Ti alloys followed parabolic kinetics. Parabolic rate constants were represented by an Arrhenius expression.

$VO_2$  is the predominant phase in the oxide scale in specimens exposed to low- $pO_2$  environments; the oxide scales are continuous and tenacious.  $V_2O_5$  was the predominant phase in specimens oxidized in air and 100%  $O_2$  environments.

Hardness profiles obtained on specimens exposed for 185 h in  $pO_2$  of  $5 \times 10^{-6}$  torr at  $700^\circ\text{C}$  indicated O concentrations in the center of the specimen attained  $\approx 90\%$  of the surface concentration.



Oxygen uptake was confined to near-surface regions for specimens that were exposed for  $\approx 200$  h at 500 and 600°C.

Uniaxial tensile data obtained on specimens exposed to environments that contained various concentrations of O indicated that uniform and total elongation were significantly decreased by O uptake of the material. Specimens exposed at 700°C exhibited almost no elongation and were not influenced by either test temperature or  $pO_2$  in the exposure environment. The data presented in this paper can be used to quantitatively assess the effect of O uptake on the tensile properties of Alloys 44 and 55 as a function of temperature, exposure environment, and section thickness.

### **Acknowledgments**

This work was supported by the U.S. Department of Energy, Office of Fusion Science, under Contract W-31-109-Eng-38. W. K. Soppet assisted with the tensile tests and D. L. Rink assisted with microstructural analysis of the oxidized and tensile-tested specimens.

### **References**

- [1]. K. Natesan and W. K. Soppet, Proc. 2nd Intl. Conf. Heat Resistant Materials, eds. K. Natesan, P. Ganesan, and G. Lai, ASM International, Materials Park, OH, 375-380, 1995.
- [2]. K. Natesan and W. K. Soppet, J. Nucl. Mater. 233-237, 482-487, 1996.
- [3]. M. Uz, K. Natesan, and V. B. Hang, J. Nucl. Mater. 245, 191-200, 1997.
- [4]. K. Natesan, W. K. Soppet, and M. Uz, J. Nucl. Mater. 258-263, 1476-1481, 1998.

Table 1. Composition of V-Cr-Ti alloys used in oxidation study.

Alloy designation	Heat identification	Composition					
		V (wt.%)	Cr (wt.%)	Ti (wt.%)	O (ppmw)	N (ppmw)	C (ppmw)
44	832665	92.7	3.50	3.54	360	73	400
55	820630	91.0	4.28	4.48	480	74	200

Table 2. Oxidation parameters of V-4Cr-4Ti and V-5Cr-5Ti alloys at various O pressures.

Oxygen pressure (torr)	T (°C)	V-4Cr-4Ti			V-5Cr-5Ti		
		$k_p$ ( $\text{mg}^2\text{mm}^{-4}\text{h}^{-1}$ )	$k_o$ ( $\text{mg}^2\text{mm}^{-4}\text{h}^{-1}$ )	Q (kJ/mol)	$k_p$ ( $\text{mg}^2\text{mm}^{-4}\text{h}^{-1}$ )	$k_o$ ( $\text{mg}^2\text{mm}^{-4}\text{h}^{-1}$ )	Q (kJ/mol)
$5 \times 10^{-6}$	500	$1.6 \times 10^{-7}$	$8.6 \times 10^4$	174	$1.3 \times 10^{-7}$	$1.4 \times 10^4$	168
	600	$3.1 \times 10^{-6}$			$2.1 \times 10^{-6}$		
	700	$4.1 \times 10^{-5}$			$3.4 \times 10^{-5}$		
$5 \times 10^{-4}$	500	$1.3 \times 10^{-7}$	$3.9 \times 10^5$	185	$1.1 \times 10^{-7}$	$8.8 \times 10^4$	177
	600	$3.2 \times 10^{-6}$			$2.3 \times 10^{-6}$		
	700	$4.7 \times 10^{-5}$			$3.0 \times 10^{-5}$		
$1 \times 10^{-1}$	500	$4.0 \times 10^{-8}$	$9.9 \times 10^5$	199	$3.6 \times 10^{-8}$	$4.8 \times 10^5$	195
	600	$1.7 \times 10^{-6}$			$9.4 \times 10^{-7}$		
	700	$2.2 \times 10^{-5}$			$1.8 \times 10^{-5}$		
160 (air)	400	$1.4 \times 10^{-7}$	$2.2 \times 10^2$	120	$8.9 \times 10^{-8}$	$2.3 \times 10^3$	137
	500	$1.1 \times 10^{-6}$			$7.1 \times 10^{-7}$		
	575	$1.2 \times 10^{-5}$			$4.6 \times 10^{-6}$		
	620	$2.5 \times 10^{-5}$			$9.0 \times 10^{-5}$		
760	450	$2.6 \times 10^{-8}$	$1.5 \times 10^9$	231	$1.8 \times 10^{-8}$	$1.5 \times 10^{10}$	247
	525	$1.6 \times 10^{-6}$			$1.7 \times 10^{-6}$		
	600	$1.9 \times 10^{-5}$			$2.0 \times 10^{-5}$		

Table 3. Phases identified<sup>a</sup> in V-base alloys by X-ray diffraction<sup>b</sup> analysis.

Oxygen pressure (torr)	Temperature (°C)	V-4Cr-4Ti	V-5Cr-5Ti
$5 \times 10^{-6}$	500	VO <sub>2</sub> , TiV <sub>4</sub> O <sub>10</sub>	VO <sub>2</sub> , V <sub>2</sub> O <sub>4</sub>
	700	VO <sub>2</sub> , V <sub>16</sub> O <sub>3</sub> , CrV <sub>2</sub> O <sub>6</sub>	V <sub>2</sub> O <sub>5</sub> , V <sub>5</sub> O <sub>9</sub> , V <sub>16</sub> O <sub>3</sub>
$5 \times 10^{-4}$	600	VO <sub>2</sub> , V <sub>2</sub> O <sub>4</sub> , CrVO <sub>4</sub>	VO <sub>2</sub> , V <sub>2</sub> O <sub>4</sub> , CrVO <sub>4</sub>
	700	VO <sub>2</sub> , V <sub>2</sub> O <sub>4</sub> , CrVO <sub>4</sub>	VO <sub>2</sub> , V <sub>2</sub> O <sub>4</sub> , CrVO <sub>4</sub>
0.1	600	VO <sub>2</sub> , V <sub>2</sub> O <sub>4</sub>	VO <sub>2</sub> , V <sub>2</sub> O <sub>4</sub> , CrVO <sub>4</sub>
	700	VO <sub>2</sub> , V <sub>2</sub> O <sub>4</sub> , CrVO <sub>4</sub>	VO <sub>2</sub> , V <sub>2</sub> O <sub>4</sub> , CrVO <sub>4</sub>
760	375	V <sub>2</sub> O <sub>5</sub> , V <sub>2</sub> O <sub>3</sub> , V <sub>3</sub> O <sub>7</sub>	V <sub>2</sub> O <sub>5</sub> , VO <sub>2</sub> , V <sub>2</sub> O <sub>4</sub>
	600	V <sub>2</sub> O <sub>5</sub> , V <sub>2</sub> Ti <sub>3</sub> O <sub>9</sub> , VO <sub>2</sub>	V <sub>2</sub> O <sub>5</sub> , VO <sub>2</sub>

<sup>a</sup>Phases identified in all samples oxidized in air (pO<sub>2</sub> = 160 torr) were primarily V<sub>2</sub>O<sub>5</sub>.

<sup>b</sup>X-ray diffraction unit was run at 1 °C/min.

Table 4. Effects of pO<sub>2</sub> on uniform and total tensile elongation.<sup>a</sup>

pO <sub>2</sub> in exposure environment (torr)	V-4Cr-4Ti		V-5Cr-5Ti	
	Uniform elongation	Total elongation	Uniform elongation	Total elongation
Exposure temperature 500°C				
1 x 10 <sup>-6</sup>	0.127, 0.147	0.217, 0.238	0.175	0.285
	-	-	0.087 <sup>b</sup>	0.155 <sup>b</sup>
7.6 x 10 <sup>-4</sup>	0.110	0.145	-	-
0.1	0.133, 0.136	0.202, 0.204	0.152	0.230
	-	-	0.087 <sup>b</sup>	0.143 <sup>b</sup>
0.15 (He)	0.140	0.191	-	-
	0.089 <sup>b</sup>	0.119 <sup>b</sup>	-	-
1.0	0.148	0.208	-	-
160	0.125	0.150	0.035	.035
	0.099 <sup>b</sup>	0.135 <sup>b</sup>	-	-
760	0.148	0.208	-	-
Exposure temperature 700°C				
1 x 10 <sup>-6</sup>	0.003	0.021	0.001	0.008
	0.0005 <sup>b</sup>	0.0009 <sup>b</sup>	-	-
0.1	-	-	0.0015 <sup>c</sup>	0.0015 <sup>c</sup>
0.15 (He)	samples broke		-	-

<sup>a</sup>Exposure time was ≈250 h; specimen thickness, 1 mm; and postexposure tensile tests were at room temperature unless otherwise indicated.

<sup>b</sup>Tested at 500°C.

<sup>c</sup>Tested at 700°C.

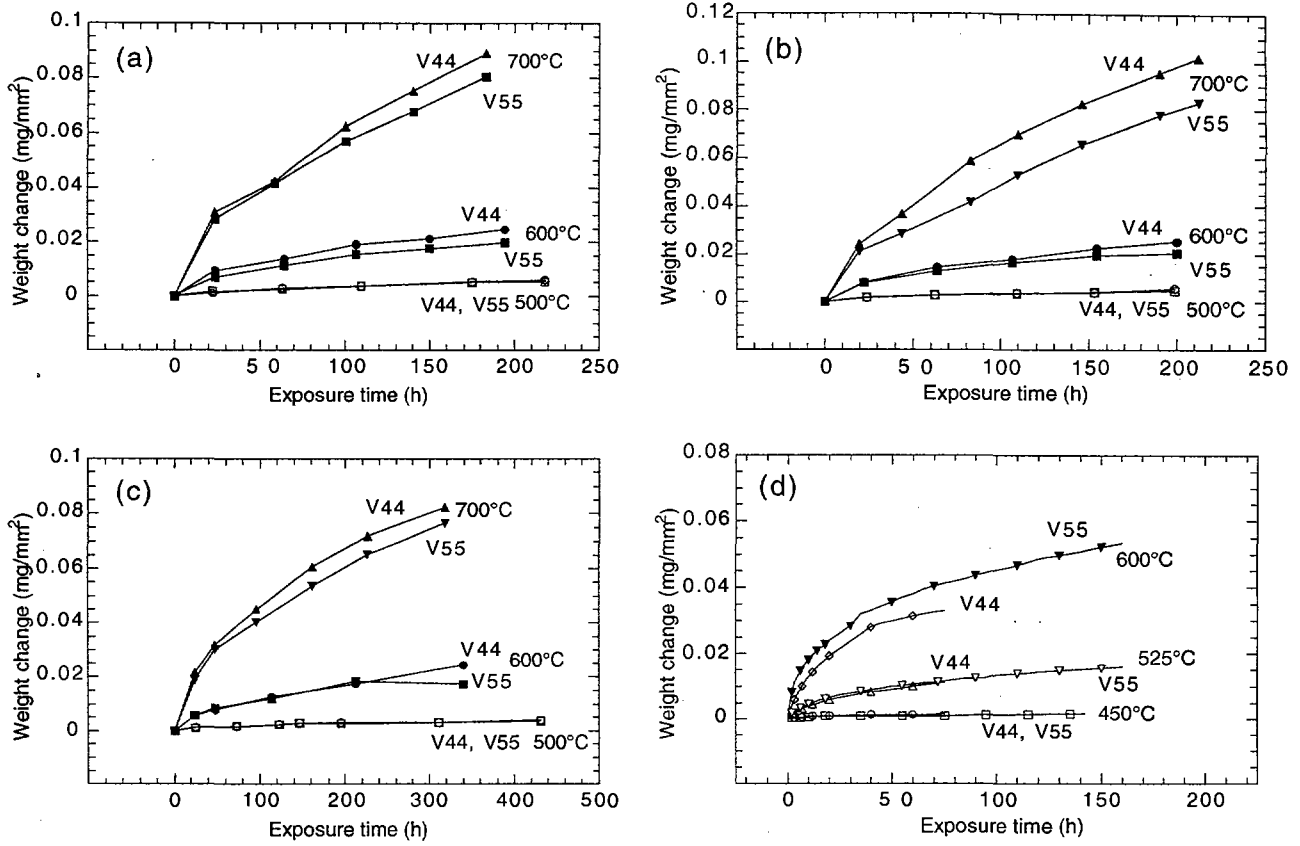


Fig. 1. Weight change data for Alloys 44 and 55 after exposure in O environments at (a)  $5 \times 10^{-6}$ , (b)  $5 \times 10^{-4}$ , (c) 0.1, and (d) 760 torr at various temperatures.

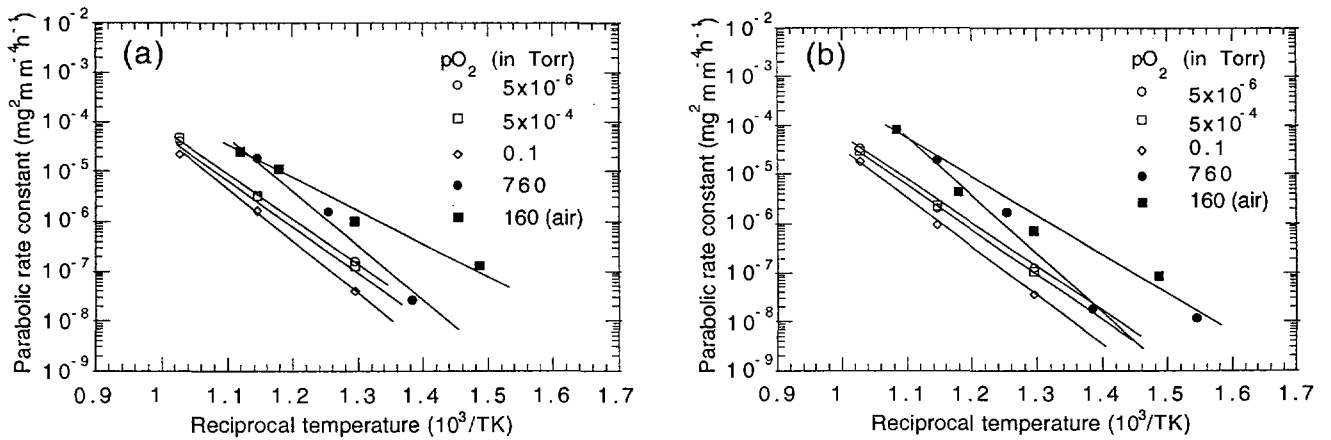


Fig. 2. Temperature dependence of parabolic rate constant for O uptake of Alloys (a) 44 and (b) 55 alloys in several low- $pO_2$  and air environments.

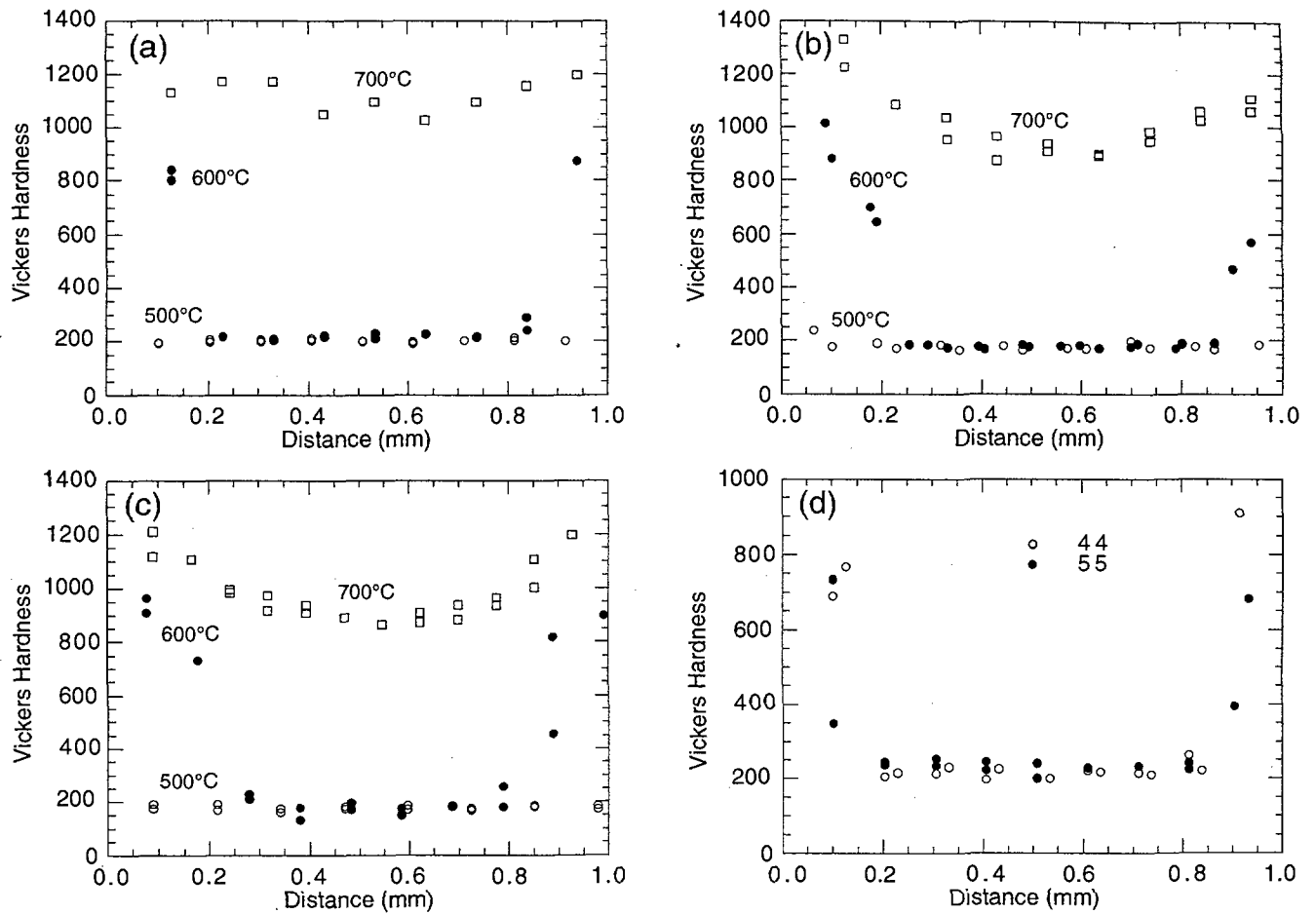


Fig. 3. Vickers hardness profiles of Alloy 44 after exposure in  $O$  environments at (a)  $5 \times 10^{-6}$ , (b)  $5 \times 10^{-4}$ , and (c) 0.1 torr at 500, 600, and 700°C, and (d) of Alloys 44 and 55 in 760 torr  $O_2$  at 600°C.